Available online at www.sciencedirect.com
ScienceDirect
Sensors and Actuators B 121 (2007) 282–294
SENSORS AND ACTUATORS B CHEMICAL
www.elsevier.com/locate/snb

The potential for and challenges of detecting chemical hazards with temperature-programmed microsensors

D.C. Meier, J.K. Evju, Z. Boger, B. Raman, K.D. Benkstein, C.J. Martinez, C.B. Montgomery, S. Semancik *

Chemical Science and Technology Laboratory, National Institute of Standards and Technology (NIST), 100 Bureau Drive MS8362, Gaithersburg, MD 20899-8362, USA

Available online 7 November 2006

Abstract

Several recent demonstrations of the abilities of micro-electromechanical systems (MEMS)-based microsensor technology to detect hazardous compounds and their simulants in a variety of background conditions are presented. In each case, two pairs of conductometric metal oxide sensors (TiO_2 and SnO_2) produced via chemical vapor deposition are operated using temperature-programmed sensing (TPS). NIST microdevices can utilize this operating mode to sample a wide operating temperature range (50 °C–480 °C) in a very short time (<15 s). The voluminous databases generated by this method can be analyzed using signal processing techniques, such as artificial neural networks (ANNs), to provide actionable outputs.

Several examples are presented: cyclohexyl methyl methylphosphonate (CMMP), a simulant for cyclosarin (GF), is detected at concentrations ranging from 700 pmol/mol to 90 nmol/mol in air backgrounds ranging from 0% relative humidity (RH) to 70% RH. The chemical warfare agents (CWAs) tabun (GA), sarin (GB), and sulfur mustard (HD) are detected at 25 nmol/mol in dry air, humidified air (40% RH), and diesel fume-laden air (3.5% saturation). Finally, a selection of five toxic industrial chemicals (TICs) and one chemical warfare simulant (CWS) are measured at immediate danger to life and health (IDLH) and permissible exposure limit (PEL) levels in an array of backgrounds, including seven different interferences, each at three concentration levels (from 0.1% to 2.0% saturation), with humidity ranging from 50% RH to 90% RH, and ambient temperature spanning 0 °C–40 °C. Technical developments that have enabled the illustrated performances, as well as future directions for conductometric microsensor research aimed at meeting the various stringent demands faced in the hazardous chemical detection application sector, are described.

Keywords: Chemical gas microsensor; Metal oxide; Chemical warfare agent; Toxic industrial chemical; Conductance; Interference

1. Introduction

Chemical hazard detection presents an array of unique challenges to analytical instrument/sensor developers. In order to provide dependable detection for hazardous analytes under real-world conditions, a detector must possess the following characteristics: sensitivity to many classes of hazards at sub-hazardous concentrations, selectivity to these analytes while in the presence of common benign compounds that may be present at a broad range of concentrations, flexible operability to account for changes in ambient temperature and humidity, and response times short enough to permit the employment of effective countermeasures to neutralize the threat. In addition to these considerations, the nature of security applications compels additional specifications, such as network deployability for the protection of more expansive facilities or perimeters, and price and power budgets sufficient to make the total cost of deployment of a system that includes all of the aforementioned features financially feasible.

A variety of chemical detection technologies are currently deployed for hazards detection [1,2]. Established technologies such as ion mobility spectrometry (IMS) [3], surface acoustic wave (SAW) devices [4,5], gas chromatography (GC) [6], mass spectrometry (MS) [7], higher-order mass spectrometry (MS–MS, MS^n) [8], other hyphenated analytical techniques (e.g., GC–MS [9], GC–SAW [10], or IMS–MS [11,12]), electrochemical devices [13,14] and chemiresisitors [15,16] are continuously being studied and improved for security applications. The advent of other technologies, such as fluorescent dyes [17], fluorescent conjugated polymers [18], and fluorescent

* Corresponding author. Tel.: +1 301 975 2606; fax: +1 301 869 5924.
E-mail address: stephen.semancik@nist.gov (S. Semancik).

0925-4005/$ – see front matter © 2006 Elsevier B.V. All rights reserved.
doi:10.1016/j.snb.2006.09.050

microbead arrays [19], promises to create additional detection methods to augment the array of existing technologies. Many of these technologies have been demonstrated to be sensitive to relevant quantities of the analytes of interest. Few studies, however, demonstrate how an analytical tool's detection capability is affected by environmental interferences, co-analytes, or changes in ambient conditions (although notable exceptions exist, e.g., [15]). Finally, the cost of currently available technology, exceeding several thousand dollars per instrument [4,20], can serve to render deployment in large-scale routine operations prohibitive.

In order to meet the requirements of security applications, the National Institute of Standards and Technology (NIST) has been performing chemical gas sensor research featuring a micro-electromechanical systems (MEMS)-based, rapid temperature-programmable, solid-state, microarray device that employs electrical conductance measurements on semiconducting metal oxide films as its basis for detection. The approach demonstrates that the use of advanced materials, advanced MEMS platforms, and advanced signal processing can be an effective approach toward meeting these analytical problems. This paper describes the sensor technology and further describes some of the issues faced in attempting to develop microsensor-based methods for chemical hazard detection.

2. Experimental

2.1. Compound classes considered

The general category of toxic compounds is not narrowly defined in terms of physical and chemical properties; in fact, harmful compounds range in size and vapor pressure from light compounds, which possess vapor pressures exceeding that of ambient atmospheric pressure (e.g., arsine) to larger, non-volatile molecules (e.g., ethyl parathion). The most dangerous compounds, such as chemical warfare agents (CWAs), can be harmful at concentrations on the order of pmol/mol. On the other hand, many toxic chemicals produced for industrial purposes only pose a health hazard at higher concentrations. In either scenario, the capability to detect sub-lethal concentrations is driven by the need for early-warning instruments. Table 1 shows the physical and chemical properties of the target compounds of the studies presented here that illustrate the scope of security detection problems. The ability to detect such target analytes in mixtures composed of a variety of interferences that can be as much as 10^8 more concentrated than the target requires detection technologies that can find a "chemical needle" in a "chemical haystack".

2.2. Microhotplate platform

The core hardware component of the NIST microsensor technology is the temperature-controlled MEMS platform shown in Fig. 1. This microhotplate platform has been discussed in greater detail elsewhere [21,22]; briefly, these devices consist of small (50 μm to 100 μm across) multilayer structures released from the substrate by top-side chemical-etch micromachining. This results in a suspended structure with an embedded doped polysilicon resistor and surface electrodes. Electrical power applied through the resistor is dissipated as heat; less than 30 mW elevates the device temperature to 500 °C within milliseconds. Using the surface electrodes, electrical properties of films on the surface can be measured independently of the heater mea-

Table 1
Hazardous compounds, their vapor pressures, and their immediate danger to life and health (IDLH) levels

	Chemical formula	Vapor pressure at 25 °C (kPa)	IDLH (μmol/mol)
Chemical warfare simulants (CWSs) and chemical warfare agents (CWAs)			
DMMP (GB)	$C_3H_9O_3P$	0.16	N/A
CMMP (GF)	$C_8H_{17}O_3P$	N/A	N/A
GA	$C_5H_{11}N_2O_2P$	0.009	0.015
GB	$C_4H_{10}FO_2P$	0.39	0.0015
HD	$C_4H_8CI_2S$	0.015	0.12
Toxic industrial chemicals (TICs)			
Acrylonitrile	C_3H_3N	14.37	85
Arsine	AsH_3	>100	3
Hydrogen cyanide	HCN	≈100	50
Methyl isocyanate	C_2H_3NO	46.4	3
Parathion	$C_{10}H_{14}NO_5PS$	0.00005–0.09*	0.8

For chemical warfare simulants (CWSs), the chemical warfare agent (CWA) the compound is intended to simulate is provided parenthetically.
* The vapor pressure for ethyl parathion is provided as a range, since its vapor pressure is strongly dependent upon the purity of the source.

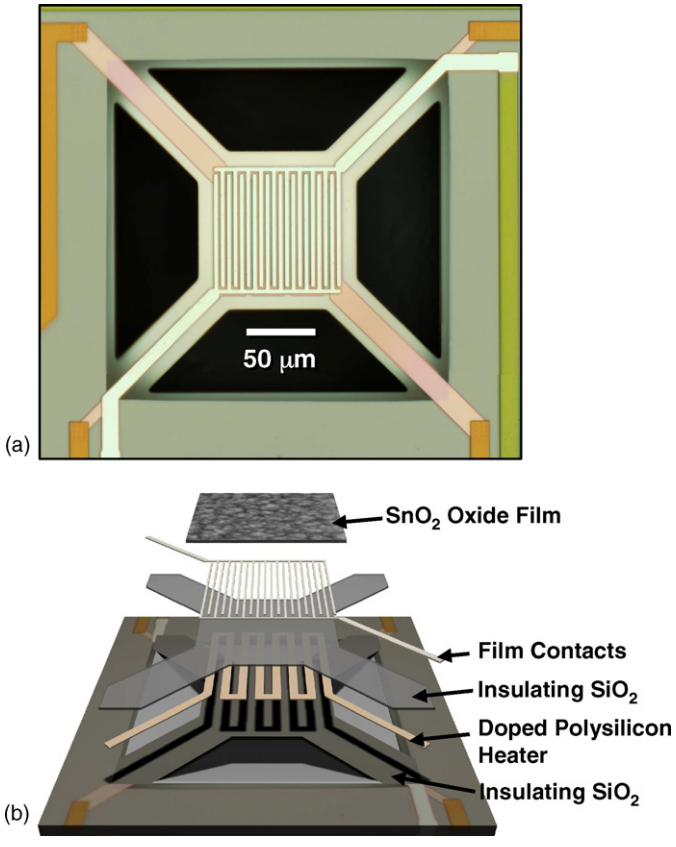

Fig. 1. An optical micrograph of a single microsensor element (a). A lift-away diagram of each layer in the structure (b).

surement and control. Replication of equivalent devices is used to produce arrays of independently controlled and measured sensors; the NIST microsensor has been previously manufactured in arrays of up to 36 independent elements. Microarrays consisting of up to 16 elements can be readily wire-bonded into 40-pin dual in-line packages, after which they can be interchangeably operated with a number of custom microsensor control and measurement electronics units.

2.3. Analyte delivery, control and containment

For tests at NIST, a custom gas delivery manifold was used to separately deliver four analyte stream components: target-laden zero-grade dry air, interference-laden dry air, humid air, and balance dry air. The manifold features non-reactive tubing for each input stream connected to a central cell, where sample blending and sensor testing occurred at essentially the same point. This manifold delivered metered concentrations of analyte either from preblended commercial cylinders (for more stable compounds possessing higher vapor pressures, such as hydrogen cyanide) or from analyte generators loaded with calibrated permeation vessels (for more reactive, low vapor pressure species such as methyl isocyanate). Depending upon the concentration of the source vessel or generator, delivered analyte concentrations ranging from hundreds of nmol/mol to hundreds of μmol/mol have been achieved. Interference vapors were introduced by bubbling metered quantities of dry air through vessels containing the interference candidate, after which the saturated gas stream was delivered via dedicated lines to the central cell (thus interferences are reported in percent saturation). In order to reduce problems stemming from fractional evaporation of interference mixtures, the liquid sources were changed out regularly. Interference introduction was performed using this method for concentrations of up to 5% saturation at room temperature. Humid air was generated by metering zero-grade dry air through a dew point generator. Test cell humidity could thus be varied between 0% relative humidity (RH) and 90% RH at 25 °C using this apparatus. Finally, balance dry air was delivered to the central cell in order to maintain constant total flow through the test system, preventing biases due to flow rate changes when any of the other three delivery lines were adjusted. The sum total flow rate of these four "single-component" streams into the central cell was generally 1 standard liter per minute (slm) or lower. For CWA tests, collaboration with a surety laboratory was required. The CWA detection experiments were performed in collaboration with the Edgewood Chemical Biological Center (ECBC). Gas delivery hardware similar to that used at NIST was installed at ECBC, where analytes were generated and verified by ECBC staff [22].

3. Technical approach overview

3.1. Sensing media—chemical vapor deposition (CVD) metal oxide thin films

Chemical detection technologies rely upon the measurement of fundamental and unique properties of different target analytes, enabling analyte identification. The NIST microsensor functions via interactions of the analyte with thin film sensor surfaces. The measured property is the thin film electrical conductance, which is a function of the analyte identity, analyte concentration, and surface temperature. Rapid temperature modulation is used to greatly enrich the microsensor data response [23].

Virtually any sufficiently conductive material that adheres to the contacts on the microdevice is a candidate sensing medium. A number of materials and nanostructures have been used, including conductive polymers [24], simple [25] and complex [26] metal oxide nanoparticle structures, and metal oxide thin films prepared by chemical vapor deposition (CVD) [22,27]. For the present work, CVD metal oxide films were chosen. The metal oxides are easy to apply to selected microhotplate elements in an array. Because the deposition process is thermally activated, the single-source precursor vapors for SnO_2 and TiO_2 (tin(IV) nitrate and titanium(IV) isopropoxide, respectively) delivered in a low-pressure environment react only at the powered (375 °C) microhotplate element (Fig. 2). While CVD fabrication generates sensing films that are more compact and less sensitive than certain of the nanoparticle-based approaches that have been used [26], device-to-device reproducibility and baseline conductances tend, at this writing, to be superior for CVD films. Second, CVD metal oxides rapidly reach stable equilibria and are usable over the entire temperature range of the microsensor device, as opposed to polymer films, which are restricted in their useful temperature range (limited by glass transitions and thermally driven oxidation or other degradation). The importance of this property will be more apparent as the microsensor operating mode, temperature-programmed sensing (TPS), is described below.

3.2. Temperature-programmed sensing (TPS)

The microsensor devices described above can function essentially as miniature Taguchi-type [28] sensors: the sensitive metal oxide film can be maintained at a desired operational temperature while the film conductance is monitored. Detection is achieved via measured conductance changes resulting from analyte introduction. While this mechanism can work well for detection problems involving a single analyte in a constant background, hazardous chemicals detection typically requires methods with multi-analyte, multi-component capabilities. Since metal oxide films generate a rather non-selective single output value, multiple sensors utilizing different steady-state temperatures and a variety of sensitive films would be required to provide orthogonal data response sets necessary to distinguish one analyte from another. As the number of potential targets and interferences increases, the number of different sensors required to generate unique responses for all possibilities could become problematic. With the NIST microsensor, however, required analytical response density can usually be achieved by using high-throughput data generated via TPS.

In TPS mode, the rapid thermal time constant of the microhotplates is used to sample the entire available temperature range of the device within a few seconds. With millisecond thermal time constants, cycling through a series of temperature steps lasting

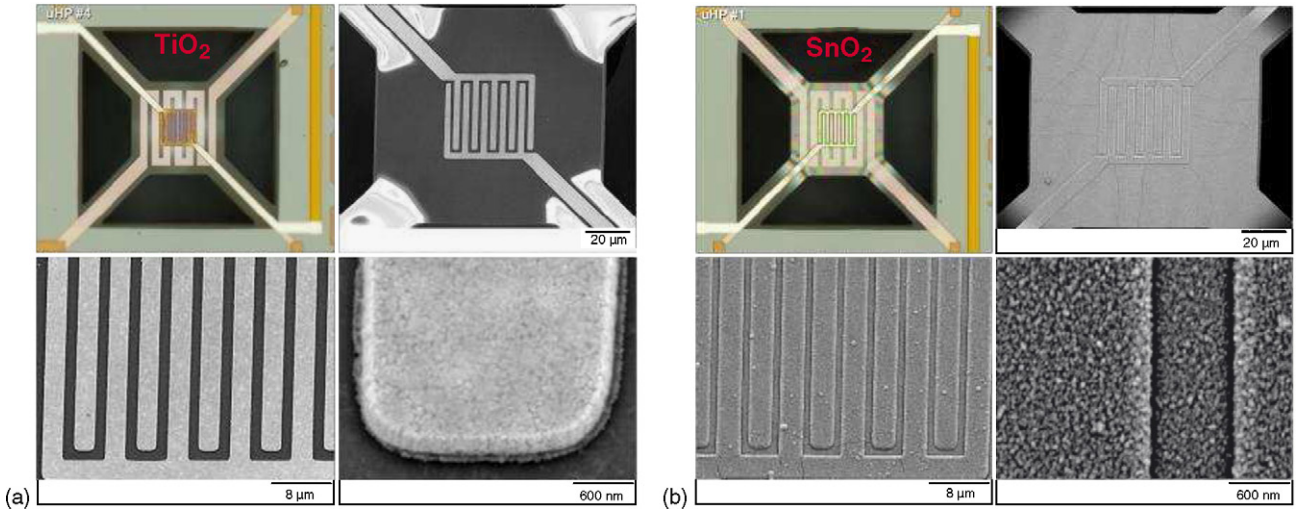

Fig. 2. Optical and scanning electron microscopy (SEM) images of individual sensor elements on the same array coated with the two sensing films used in this work, (a) titanium oxide (TiO_2) and (b) tin oxide (SnO_2).

on the order of 100 ms per step allows for separate conductance measurements of the sensing film at each step. Fig. 3 shows two such TPS programs. The program in Fig. 3a cycles between a linear temperature ramp and a constant base temperature; more complex programs, such as the one shown in Fig. 3b, can be used to enhance certain features of the program. In this case, designing a ramp concave toward lower temperatures reduces the total energy expended in driving the sensor. Furthermore, applying such a ramp, then applying its mirror image, results in different measurements at corresponding temperatures due to short-term history effects. Finally, the selection of different cycling baseline temperatures for each half of the program is intended to change the signal in corresponding temperature points due to changes in the analyte adsorption, desorption, and reaction character at different temperatures. The resulting data stream contains a conductance measurement for each sensor in the array at each temperature point. Depending upon the sensing film selection and the temperature program chosen, the data array could exceed several hundred points per TPS cycle, collected in on the order of 10 s. From such arrays, it is possible to extract identifying information for a variety of compounds and mixtures simulataneously, and to do so on time scales relevant to security applications, such as early warning.

3.3. Challenging the sensor

To determine detector sensitivity, speed, and selectivity under a variety of conditions, certain critical aspects of the testing apparatus must be considered. First is the purity and reproducibility of analyte reaching the sensor; second is the reliable generation of known quantities of interference mixtures and compounds, ranging from simple water vapor to a variety of petroleum distillate mixtures and cleaning products. Due to incompatibilities of a number of these compounds with other gases and with plumbing hardware (chemical hazards in many cases owe their lethal properties to their high reactivity), it is imperative that gas delivery materials be selected to minimize interactions, and that well-defined detection tests occur as soon as possible after blending to reduce measurement uncertainty due to side reactions (allowing the association of a particular response with a defined chemical ambient). An apparatus that permits measurement near (within 20 mm) the point of analyte blending also allows for more careful chemical fate analysis through comparisons of signals at the described point-of-mixture (upstream) and at another location down the exhaust line (downstream). Such comparative studies help to determine device performance when decomposition products dominate the analyte stream, and provide

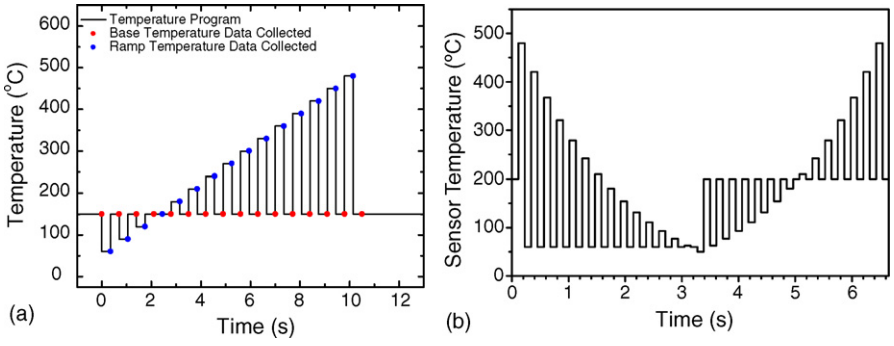

Fig. 3. Sample temperature-programmed sensing (TPS) operation profiles. Program (a) was used in CWA measurements, while TIC and CWS experiments utilized program (b).

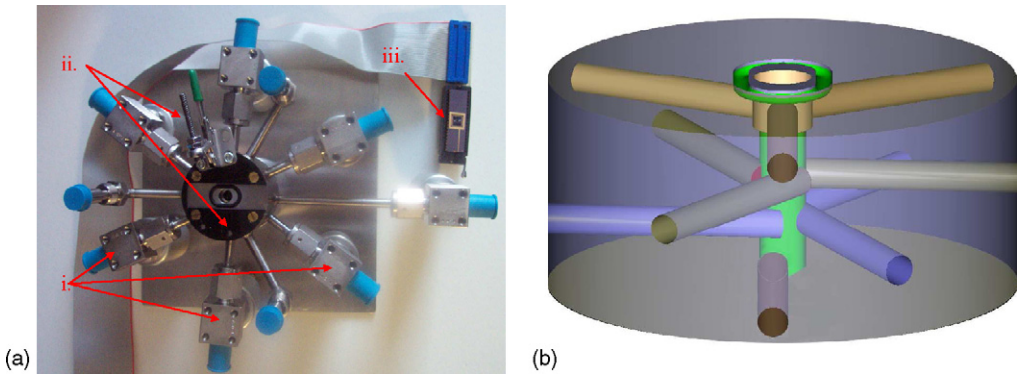

Fig. 4. A multiport flow cell designed to rapidly assess the microsensors' detection capabilities for a given analyte at a variety of test conditions. An assembled cell (a) contains: (i) computer-controlled pneumatic valves to control flow on/off for each analyte mixture component (mounting valves as closely as possible to the test cell reduces system response time); (ii) a capture plate and locking mechanism to ensure reproducible placement of, and a tight seal to, the sensor package; and (iii) a packaged NIST microsensor array is shown for reference. The cut-away view of the cell (b) shows the off-axial orientation of the input flow lines, which aids the blending of the different input flows by generating turbulence.

information for instrument adjustments that account for such decomposition.

The central cell for our hazard studies was designed to best enhance mixing and flow in this system. In order to switch as rapidly as possible between challenge conditions (defined as a background composition, ambient temperature, and analyte concentration), it was necessary to make the cell volume small. The cell volume was roughly 10 cm^3, resulting in an analyte residence time of less than 1 s. This is shorter than our typical TPS program time, and produces clear distinction between analyte challenge states in the sensor signal. To further serve the goal of rapid analyte state switching, flow for each of the single-component streams was held constant in both concentration and flow rate prior to delivery to the cell. To both maintain a sharp, clear introduction of components and to minimize diffusion of previously delivered components from dead space volumes leading to the main cell, the delivery control valves were mounted as closely as possible to the mixing cell. Three-way valves were used, and most lines continued to flow gas in a bypass mode even when not being measured directly by microsensors, in order to prevent concentration spikes from pressurized lines or lagging analyte delivery. Valves were switched pneumatically using a computer-controlled switchboard; software control made experiment reproduction and timing routine. Finally, the cell itself was machined from 304 stainless steel with seven inlet ports (one each dedicated for target, humidity, and balance air; the remaining four were used for interferences). Mixing within the cell is aided by the off-axial orientation of the inlets. An assembled test cell, along with its internal geometry, is shown in Fig. 4.

3.4. Signal processing methods

Very large, relatively complex databases like those generated by TPS-operated microarrays require advanced signal processing methods to efficiently extract the most critical information from the data and transform it into a simple, single, actionable output. The task at hand is yet more difficult when considering applications involving multi-target and multi-background environments. Due to these complexities, artificial neural networks (ANNs) were employed. In previous microsensor work [29,30], ANNs have been shown to provide rapid classification of data into distinct categories. For the purposes of this work, classification into "target present" and "target absent" states fulfills the output requirements for security and early warning applications. Quantification of analytes is also possible using ANN, as has been demonstrated previously [31,32].

A schematic of the data processing method is shown (Fig. 5). Briefly, the data generated during any single TPS cycle is presented to a network comprised of a matrix of initial connection weights (which roughly translates into an estimate of the effect that a given data point's value has on the outcome), hidden neurons (which allow for correlation of data within the input set and allow the network to draw non-linear relations between the inputs and the outputs), and an output value. Reiterative fine adjustment of the connection weights and re-presentation of the data results in a network that provides the highest probability of the correct output for a given set of inputs. Following this insector training step, which is performed off-line using a subset of the data stream, a validation step in which all of the data is presented to the trained ANN is performed. The robustness of the model and the speed of the sensor response are evaluated based upon the results generated from the process. This application of ANN and statistical methods to confirm the value of the sensor data is diagrammed below in Fig. 5.

4. Results and discussion

4.1. Chemical warfare simulant detection

The first demonstration presented is for the detection of a chemical warfare simulant (CWS), cyclohexyl methyl methylphosphonate (CMMP), which is intended to approximate the physical properties of cyclosarin (GF) without possessing its toxicity. The array device used for this demonstration is composed of four elements consisting of pairs of TiO_2 and SnO_2 sensors. Such internal redundancy can provide valuable internal performance checks. The TPS program used to operate each element of this device is shown in Fig. 3b (29 ramp points per TPS

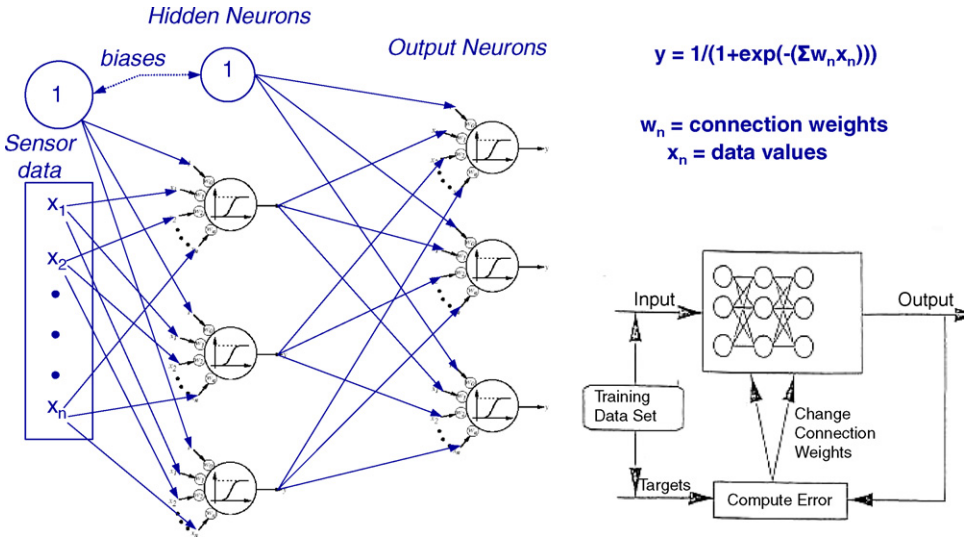

Fig. 5. A schematic of the artificial neural network (ANN) method of analyzing complex data sets such as those generated with microsensor TPS. Reiterative data presentation and connection weight adjustment produces the greatest classification efficiency.

cycle from 480 °C to 50 °C and back). Fig. 6a shows a series of conductance isotherms measured on a microsensor element with a SnO_2 sensing film during a test exposure to 40 nmol/mol and 90 nmol/mol of CMMP. Tracing any one isotherm provides data reminiscent of that generated by Taguchi-type sensors. The key (shown above the data) denotes the time sequence of the challenge program, which switches conditions every 15 min, including analyte delivery in dry air and at three different RH levels (10%, 40%, and 70%). The flow rate for this test ranged from 500 standard cubic centimeters per minute (sccm) at low-concentration analyte exposures to 250 sccm at high-concentration exposures, so that the signal contains a response to the sample flow rate as well as to the chemical environment. The conductance changes at each step are nearly immediate and readily observable, though signal relaxation occurs throughout the exposure such that steady state is not always reached. It is interesting to note the humidity-dependent response inversion with increasing analyte concentration. While the conductance measurements are higher for both analyte concentrations with respect to the background condition signal, the conductances measured at 90 nmol/mol CMMP and low humidity are lower than that for 40 nmol/mol CMMP under equivalent conditions. While this response inversion is observed under low humidity conditions, raw conductance increases with analyte concentration as the humidity level is set to 40% RH and higher. This illustrates the complexity of conductometric microsensor array signals, and highlights the benefits of training a sensor array under a range of conditions that span the expected deployment conditions, ensuring that the largest conceivable range of raw data output has been accounted for.

The raw data of Fig. 6a, along with the ramp isotherms from the other three elements (for a total of 116 temperature features in each cycle), are preprocessed by normalization to the highest conductance within each element, then presented to the ANN for training and classification. In Fig. 6b, the recognition probabilities for CMMP produced by the trained ANN are shown. The ANN probability outputs are generated from TPS cycles used for in-sector training (black) and validation (red). High probability of recognition of the CMMP is indicated by ANN probability output values near one, while low probability of target presence generates ANN outputs near zero; for this exercise, no distinction was made in the training between the high and low concentrations. The high probability of detection and recognition of CMMP under these varied conditions is illustrated by the low noise and high confidence level of the trained output; only at the highest tested humidity level is identification onset significantly delayed from the point of analyte introduction. The output demonstrates how a properly trained ANN condenses data from tens of inputs into a single-valued, actionable output representing the recognition of an analyte under a variety of background conditions.

4.2. Chemical warfare agent detection

Successful detection demonstrations have also been performed using live CWA compounds. Single analyte studies of CWAs and CWSs in zero-grade dry air have been reported previously [22,29]. For this study, the ability of a NIST microsensor array to identify CWAs in changing humidity and diesel fuel vapors was examined. A similar sensor configuration to that used in the CWS work described above was employed, although the TPS program applied was similar to that shown in Fig. 3a. For CWA applications, a detection technology must generate an alarm at extremely low concentrations in order to provide relevant information. As a result, the signal due to target analyte presence is not always immediately apparent as the concentration levels approach the limits of detection of the device. Fig. 7 shows examples of signals measured from a SnO_2 sensing film both with and without 25 nmol/mol sulfur mustard agent (HD) in dry air and 40% RH air backgrounds. These data are plotted not as isotherms, like the CMMP data shown previously (Fig. 6a), but as time-traces corresponding temporally to several cycles of the TPS program. Stack-plotting these signatures better shows the subtle conductance changes that occur upon analyte

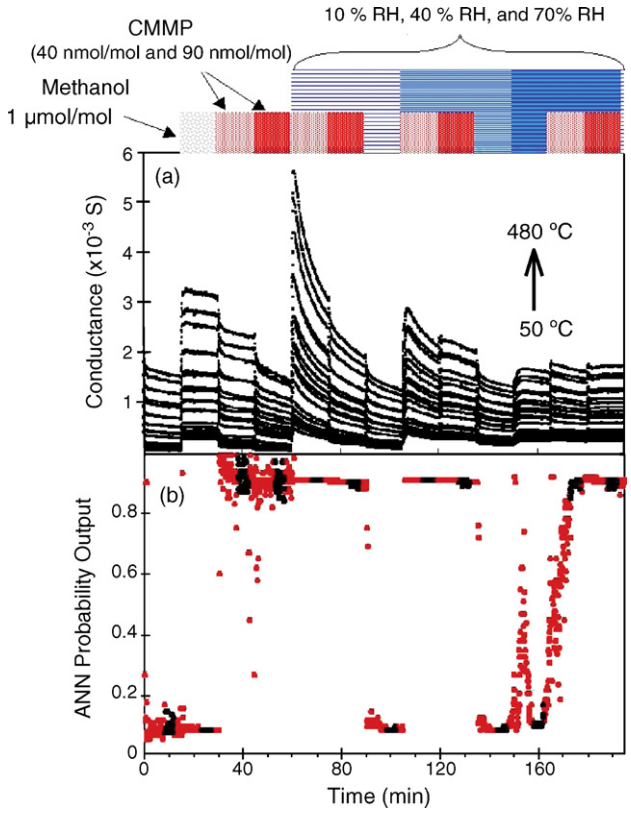

Fig. 6. CWS detection using the TPS mode. A key to the plot (top) shows the sensor challenge conditions for the raw data (top) and ANN classification results (bottom) shown. Gray denotes 1 μmol/mol methanol in dry air; the pink and red denote 40 nmol/mol and 90 nmol/mol cyclohexyl methyl methylphosphonate (CMMP, a cyclosarin (GF) simulant), respectively; the three shades of blue denote air backgrounds with 10%, 40% and 70% relative humidity (RH), respectively. (a) Conductance isotherms of a single SnO_2 sensor element during TPS data collection for the 195-min test run. (b) ANN training (black) and validation (red) probability outputs are derived from the conductance isotherms collected at each ramp point on all four sensor elements. The high probability of detection and recognition of CMMP under these conditions is illustrated by the low-noise, high-confidence ANN outputs.

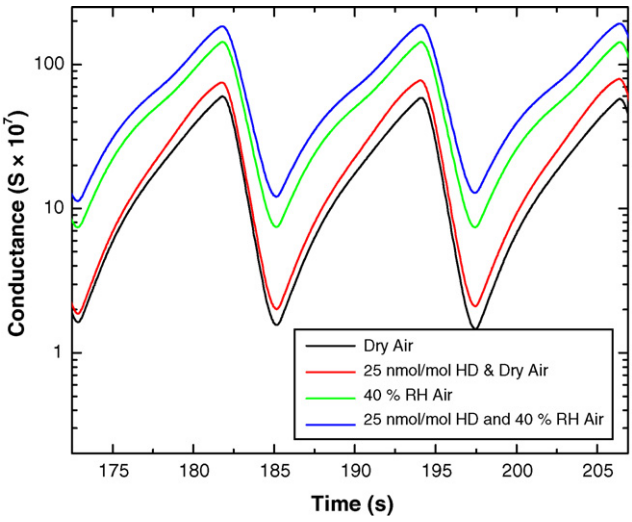

Fig. 7. An example of raw data generated using a SnO_2 sensor for sulfur mustard (HD) detection under changes in humidity. For clarity, raw data is displayed sequentially by TPS cycle (see program Fig. 3a); equivalent cycles collected from separate sections of the challenge profile are overlaid to highlight differences in the data. While the conductance signature change induced by HD exposure is subtle, it is measurable regardless of whether the humidity is 0% RH or 40% RH.

introduction. For this example, the increase in conductance corresponding to the humidity change is relatively large, while that due to HD exposure is small. However, the magnitude of the HD signal is similar under both humidity conditions, indicating that covariance in the signature due to HD-water interactions at the surface are not as pronounced over this humidity range as the effect observed for CMMP-water interactions.

The HD results, which included single-analyte exposures in dry air and co-analyte exposures in dry air with 40% RH or diesel fuel vapor at 3.5% relative saturation, along with results collected from similar experiments that challenged the sensor array with 25 nmol/mol GB or 25 nmol/mol GA in place of HD, were presented to an ANN for training and classification. The results of these analyses are provided in Fig. 8. The flow program key (at the top of the figure) summarizes the challenge; each stage contains 5 min at the basic background condition (zero-grade dry air), followed by 3 min of target presentation, then 2 min of the background condition, before advancing to the interference background condition. The analyte flow pattern is repeated, after which 2 min of the background condition is reintroduced to prepare for the introduction of the next analyte/interference combination. As described previously, probabilities near one indicate target presence while probabilities near zero indicate target absence. In this case, however, there are three independent outputs, one for each target. The validation output shown is in agreement with the target delivery schedule. While the output values are generally close to the confidence limits, it can be useful in applications to set an alarm threshold value that defines at what detection probability action will be taken. In Fig. 8, a

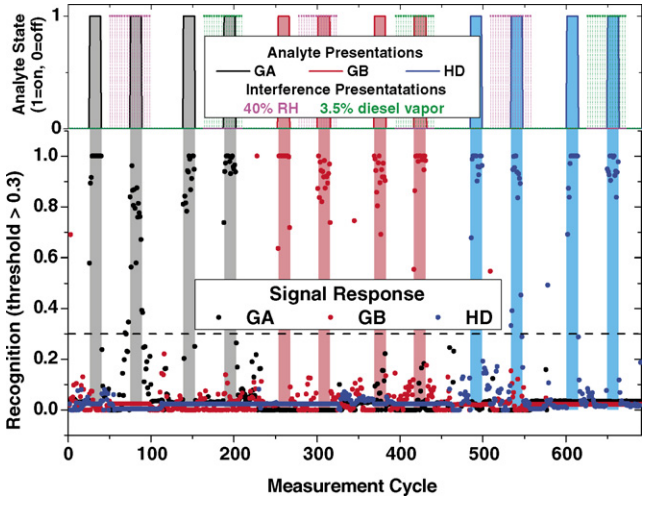

Fig. 8. Detection and identification of the CWAs tabun (GA), sarin (GB), and sulfur mustard (HD) both as single analytes in dry air and as co-analytes in air backgrounds containing water vapor (40% RH) or diesel fuel vapor (3.5% of saturation) using the ANN classification procedure. Each compound is distinguished not only from the three background conditions, but also from each other. Each measurement cycle (corresponding to the TPS program length) is approximately 12.5 s; positive identification occurs within a few cycles of condition introduction.

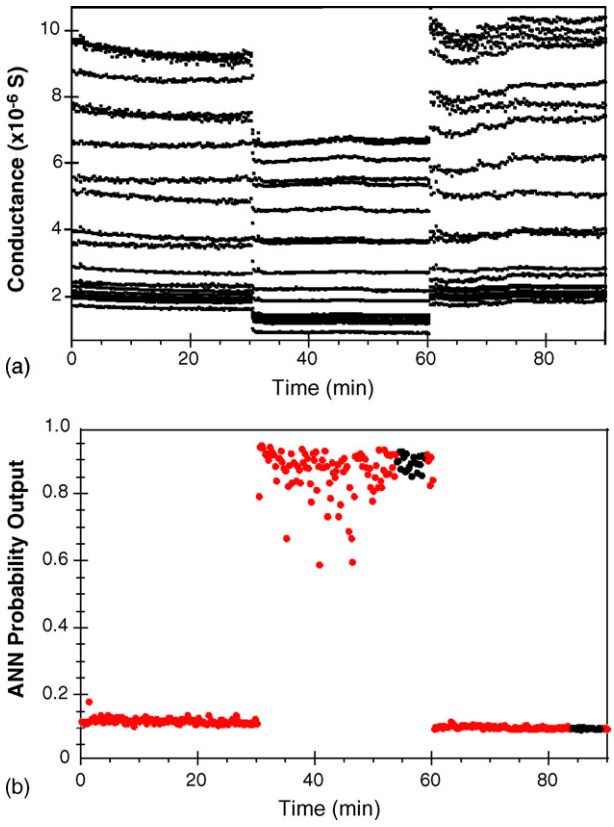

Fig. 9. A preliminary survey of CWS low-concentration data and analysis. The comprehensive raw data plot (a) shows 20 conductance isotherms of a SnO_2 sensor operated with the 29-temperature TPS program (Fig. 3a) ranging from 480 °C (highest film conductance) to 50 °C (lowest film conductance) during a test exposure to 700 pmol/mol of CMMP in a constant 40% RH air background condition. The sensor is exposed to CMMP between the 30 min mark and the 60 min mark. The ANN training (black) and probability for recognition (red) of 700 pmol/mol CMMP at 40% RH is shown in (b).

0.3 probability alarm threshold was selected. This value would result in accurate alarms for this system and these analytes; false alarms occur only at valve actuation events during the experimental measurements that liberated dead space gases and caused momentary flow and pressure changes – events that, with proper engineering, are unlikely under deployed conditions. An adjustment of this threshold probability could be made to suit the requirements of differing applications.

4.3. Exploring the limits of sensitivity for agent targets

There is particular interest in lowering the limits of detection (raising sensitivity) for certain classes of compounds, especially those used as CWAs, since detection of even the smallest amount of such compounds constitutes an actionable event. To that purpose, preliminary studies to explore the limits of microsensor sensitivity (on more easily accessible CWSs) were performed. For comparison to prior work, the target analyte demonstrated here is again the GF simulant CMMP, now delivered to the sensor at 700 pmol/mol (≈100× lower than in Fig. 6a) in air background at 40% RH. Fig. 9a shows the conductance measurements of a SnO_2 sensor [33], traced as isotherms, at 20 selected temperatures from 480 °C (highest conductance) to 50 °C within a TPS program similar to that shown in Fig. 3b. The test exposure to 700 pmol/mol of CMMP occurs between the 30 min mark and the 60 min mark, while the flow rate (2 slm) and humidity remain constant. The trained (black) and validated (red) ANN probabilities for recognition of 700 pmol/mol CMMP at 40% RH are shown (Fig. 9b). This plot is based on data collected from a 4-element sensor array consisting again of two pairs of SnO_2 and TiO_2 sensors. Due to the reduced magnitude of the sensor response to reduced target concentrations, additional data preprocessing is required for more accurate modeling.

Prior to the ANN data analysis, the data from each element was preprocessed by computing the logarithm of the conductance data, normalizing to the highest value within a single TPS cycle, and zero-centering within the same cycle. The successful detection of CMMP under these conditions is indicated by the high probability of target presence computed during the exposure (between 30 min and 60 min) and the low probability reported elsewhere.

4.4. Toxic industrial chemicals detection

High sensitivities and rapid responses have been demonstrated by results presented here for the CWA application area. However, for security applications, an attack need not necessarily involve CWAs. More readily available toxic industrial chemicals (TICs) may provide an easier means of attack than conventional CWAs. Therefore, a detection technology should be capable of measuring TICs as well as CWAs. This places additional demands on candidate detection technologies due to the large range of compounds available and their equally large range of chemical properties. It has been demonstrated previously [23] that conductometric sensors possess high sensitivity to low-molecular-weight volatile organic compounds (which have certain physical similarities to many TICs); furthermore, previous studies have shown that TPS-derived microsensor data can be used to differentiate between compounds and correctly identify compounds within mixtures [32].

In this work, the microsensors are challenged to detect and identify five TICs (hydrogen cyanide, methyl isocyanate, arsine, ethyl parathion, and acrylonitrile) and one CWS (dimethyl methylphosphonate – DMMP – a sarin (GB) simulant) at concentrations equivalent to IDLH (immediate danger to life and health, shown in Table 1) and PEL (permissible exposure limit, in these cases ranging from 20% to 1% of the IDLH levels). These tests were performed under a base condition of 50% RH and 25 °C. In addition to this base condition, tests were performed at 0 °C and 40 °C, as well as at 90% RH and 25 °C. In addition, the sensor was exposed to three levels (0.1%, 1.0%, and 2.0% relative saturation) of seven different interfering vapors – Windex, Clorox bleach, ZEP Perimeter floor stripper, Fantastik Orange Action cleaner, WD-40, gasoline (87 octane rating), and commercial #2 diesel fuel [34]. Exposures to interference conditions were sequential, alternating between target analyte presence and absence every 10 min. The sensors were configured as pairs of SnO_2 and TiO_2 sensor elements and were operated using the TPS program shown in Fig. 3b.

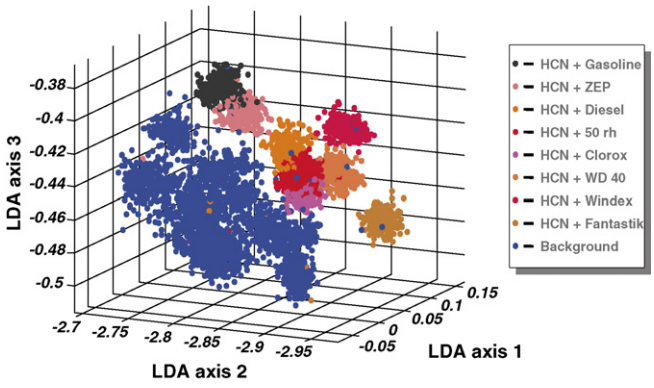

Fig. 10. Linear discriminate analysis (LDA) of raw sensor data collected during exposure to a variety of background conditions and 50 μmol/mol hydrogen cyanide, demonstrating the capability to discriminate between analyte presence and analyte absence under a broad variety of conditions.

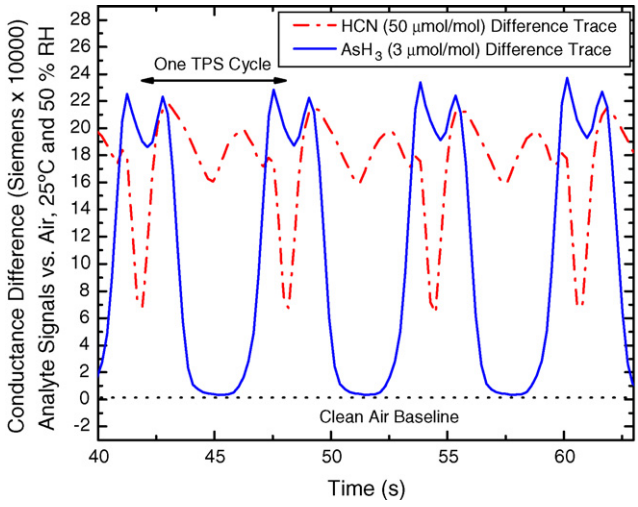

Fig. 11. Background-substracted TPS data from a single SnO_2 sensor showing that data signatures produced by hydrogen cyanide and arsine are distinguishable from each other. Corresponding data collected in air are subtracted from the raw data to enhance clarity and demonstrate signature repeatability.

When faced with a problem of this complexity, it can be helpful to determine from the raw data whether confirming analyte presence under a variety of conditions is feasible. Fig. 10 shows an example of linear discriminant analysis (LDA) [35] used to determine whether statistically significant differences between analyte states can be extracted. Each data point in the figure represents a complete TPS cycle measured during a hydrogen cyanide (HCN) challenge at 50 μmol/mol. In this case, LDA is used to find a lower-dimensional transformation that maximizes the separation between samples with HCN present and HCN absent. Within the first three LDA axes, it is readily apparent that data collected with target absent (all blue points) lie in a separate part of the transformed space than the data collected with target present (clusters of all other colors – note the key for background identification). This result shows that even complex detection problems are solvable provided sufficient dimensionality of the sensor database, i.e., measurements using more materials and a greater range of temperatures provide the possibility of improved separability.

As important as the ability to separate data signatures from their background signatures is, it is equally important to be able to distinguish between a number of different analyte signals, since appropriate countermeasures may well be dependent upon the chemicals released. Fig. 11 shows an example of a comparison between two target analytes. The hydrogen cyanide (50 μmol/mol) and the arsine (3 μmol/mol) traces are a series of TPS cycles from a SnO_2 sensor element measured in the presence of the analyte (background traces collected previously are subtracted for clarity). Not only are the traces quite repeatable, but they are also distinctly different from each other.

Having established sensitivity to, and selectivity for, two of the six small-molecule TICs in the original challenge, the ANN data processing was applied to the entire challenge set in order to determine the number of correct classifications of challenge states that could be made. A sample of this output, showing the classification results of HCN exposures at 50 μmol/mol during the interference challenges, is shown in Fig. 12. The red trace indicates target presence, with 1 being present and 0 being absent. The colored bands (identified in the key) indicate the presence of interferences – the first exposure for each interference is introduced at the lowest tested concentration (0.1% relative saturation), the second introduction is at 1.0%, the third, 2.0%. The ANN output is shown as blue points corresponding to each TPS cycle; the high correlation between the target program trace and the output indicates successful target identification. For this example, excellent agreement was observed between analyte state and ANN classification output; furthermore, these results were typical for all analytes at all conditions, with false classifications being far more the exception than the rule. The classification outcome for both the CWA demonstration (Table 2a) and the TIC demonstration (Table 2b) are tabulated. There are fewer than 3% false classifications for the entire set, and most of these occur during challenges with methyl isocyanate (a highly unstable molecule that is difficult to deliver in pure form, particularly in interference-laden and humid air) and arsine. Considering that the chemical response of conductometric metal oxides is non-specific, it appears counterintuitive that a sensor based upon such materials can provide the demonstrated degree of discrimination. It can be speculated that because of low analyte pressures and high operating temperatures, surface coverages of most analytes and interferences (with the exception of water) are relatively low. For this reason, minimal analyte-analyte and analyte–interference interactions at the surface result in minimal sensor signal covariance in most cases, generating data that contains features that are simpler to recognize.

4.5. Future directions

Microhotplate-based conductometric sensing that utilizes TPS methods to increase the analytical information of response signals has been demonstrated to be a viable approach for recognizing dangerous chemicals. However, further technological advances are necessary to expand the detection capabilities to encompass a more comprehensive list of potential analyte targets, particularly ultra-deadly compounds such as VX nerve

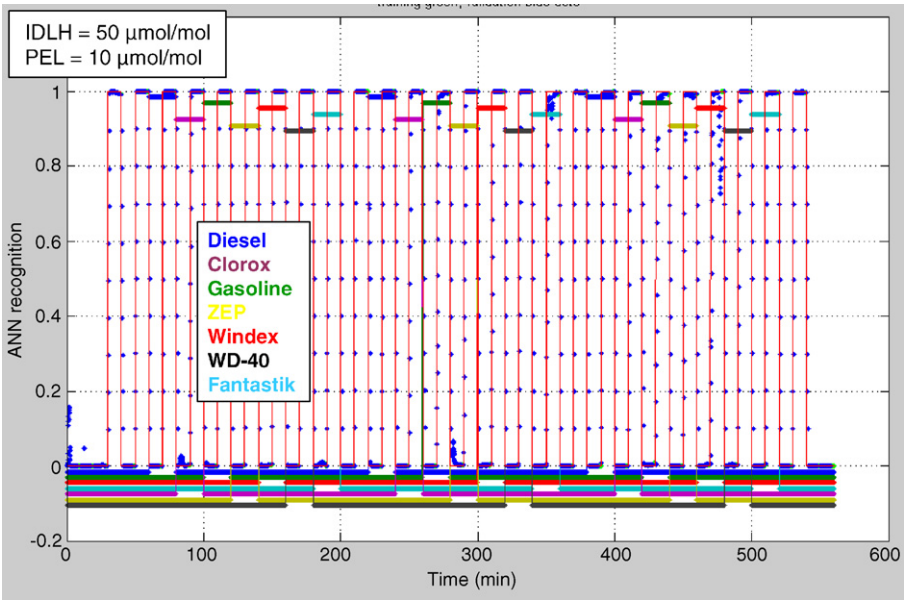

Fig. 12. ANN recognition output for a 10 µmol/mol exposure to hydrogen cyanide (HCN) followed by a series of 25 exposures to 50 µmol/mol HCN in a 50% RH air background and in the presence of seven sequentially introduced interferences at three concentration levels (0.1%, 1.0% and 2.0% of saturation levels). The red trace indicates target presence, with 1 being present and 0 being absent. The colored bands (identified in the key – mention of these and any other commercial products is strictly for proper experimental definition, and does not constitute an endorsement by NIST) indicate the presence of interferences. The ANN output is shown as blue points corresponding to each TPS cycle; the high correlation between the target program trace and the output indicates successful target identification.

agents, contraband such as narcotics, and low-volatility hazards such as explosives. The obstacles inherent in solving these problems are expected to be overcome, in part, by the design and deployment of even more sensitive sensing materials and by the integration of preconcentrators with detectors. A number of nanoscale materials (such as Sb-doped SnO_2 nanoparticle spheres and Nb-doped TiO_2 nanoparticle films, shown in Fig. 13a and b, respectively) are already being synthesized and tested for sensitivity to a suite of volatile organic compounds and small molecules. Preliminary results suggest that devices utilizing these porous materials achieve significantly higher sensitivities compared to compact CVD-derived films [26,36].

As advancements in the development of new high-sensitivity materials, specialized operational schemes, and advanced signal processing methods more fully meet the demands of reliable hazard detection, the importance of factors including reproducibility, stability, and analytical adaptability become increasingly evident. Methods for processing nanomaterial structures on the device platforms must demonstrate enhanced transduction properties while maintaining the integrity and functionality of the microdevice platforms. Nanomaterials must be fabricated and deposited under tight tolerances to ensure device-to-device reproducibility. Applying these materials to microdevices in a manner that ensures reproducible, low-resistance electrical contact is also critical. The increased sensitivity of new sensing materials can come at the price of increased susceptibility to tiny compositional or structural changes at their surfaces and interfaces, which can lead to drift. Therefore, an additional research

Table 2
Microsensor hazard detection scorecards for CWAs (a) and TICs (b)

	None (air, humidity, and diesel vapor)	GA	GB	HD
(a) CWAs				
Presentations	12	4	4	4
Correct recognition/false negatives	N/A	4/0	4/0	4/0
False positives or cross positives	0	0	0	0

	None	ACN	AsH_3	HCN	MIC	DMMP	Para
(b) TICs							
Analyte presentations (neat, interference, environmental, PEL and IDLH)	585	84	84	90	87	101	87
Correct recognition	571	84	80	90	79	100	85
False negatives or false positives	14	0	4	0	8	1	2

CWA challenges occurred at 25 µmol/mol in zero-grade dry air, 40% RH and 3.5% relative saturation of diesel vapors. TIC challenges of IDLH (immediate danger to life and health) and PEL (permissible exposure limit) concentrations occurred at 0 °C, 25 °C, and 40 °C, 50% RH and 90% RH, and under 0.1%, 1.0%, and 2.0% relative saturation of the vapors of the following common products: diesel fuel, gasoline, Clorox bleach, Windex, Fantastik Orange-Action cleaner, ZEP Perimeter floor stripper, and WD-40 penetrating oil. The target analyte abbreviations are as follows: ACN: acrylonitrile, AsH_3: arsine, HCN: hydrogen cyanide, MIC: methyl isocyanate, DMMP: dimethyl methyl phosphonate (a sarin (GB) simulant), and Para: ethyl parathion.

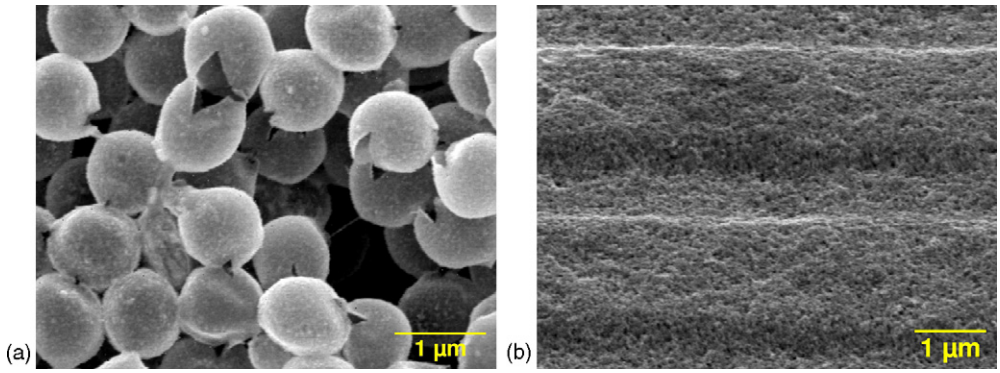

Fig. 13. SEM images of (a) Sb-doped SnO_2 nanoparticle microshells and (b) Nb-doped TiO_2 nanoparticle films adhered to NIST microsensor elements.

component within our TPS approach includes determining temperature modulation regimes that minimize such effects. Success in producing and integrating reproducible, stable and highly sensitive sensing materials for microsensor arrays will make optimizing signal processing routines easier, but challenges still exist to develop robust and transferable methods that can be applied and adapted to various hazardous gas detection application subsectors. Recognition architectures will be most valuable when they can identify and discriminate hazards using expandable and transferable libraries that properly account for a variety of background conditions. The analysis scheme should also balance library size and algorithm robustness.

Finally, the challenges of on-line, simultaneous detection of larger target analyte sets in a greater diversity of background conditions are now being met with some success through a combination of sensing materials selection, target-specific temperature programming, and dynamic and more robust signal processing. While current results demonstrating off-line recognition of data collected during the in-sector training are promising, further improvement of the data processing algorithms is required to ensure that data collected in the future will be properly recognized by machine learning techniques trained using data collected today. A baseline drift assessment of the technology is currently underway, with statistical and mathematical methods being tested for their abilities to counteract any sensor drift components. Accomplishing this goal will make passing the final test possible – detection of target analytes in real time.

5. Conclusions

The combination of advanced materials, advanced platforms, and advanced signal processing methods shows great promise for the challenges of hazard detection in realistic environments. It has been demonstrated that conductometric microsensors using artificial neural networks (ANNs) data mining techniques to extract useful information from databases generated by high-throughput temperature-programmed sensing (TPS) programs can be used to detect and identify a variety of CWSs, CWAs, and weapon-related TICs in a range of background conditions and in the presence of a variety of potentially interfering co-analytes ranging from water vapor to vapors from petroleum distillates and household cleaners.

Acknowledgments

We acknowledge the contributions from the staff of the Edgewood Chemical Biological Center (ECBC), particularly those of Michael Ellzy and J. Michael Lochner, in the CWA detection experiments. We also acknowledge technical support from Michael J. Carrier and James D. Melvin at NIST. Financial support for this work was provided by the Department of Homeland Security (DHS-HSARPA), the Defense Threat Reduction Agency (DTRA), the Department of Defense (DoD), and a Postdoctoral Research Associateship from the National Research Council (NIST-NIH-NRC).

References

[1] H.H. Hill, S.J. Martin, Conventional analytical methods for chemical warfare agents, Pure Appl. Chem. 74 (2002) 2281–2291.
[2] Y. Seto, M. Kanamori-Kataoka, K. Tsuge, I. Ohsawa, K. Matsushita, H. Sekiguchi, T. Itoi, K. lura, Y. Sano, S. Yamashiro, Sensing technology for chemical-warfare agents and its evaluation using authentic agents, Sensors Actuators B: Chem. 108 (2005) 193–197.
[3] G.A. Eiceman, J.A. Stone, Ion mobility spectrometers in national defense, Anal. Chem. 76 (2004) 390A–397A.
[4] C.M. Harris, Seeing SAW potential, Anal. Chem. 75 (2003) 355A–358A.
[5] J.W. Grate, S.L. Rose-Pehrsson, D.L. Venezky, M. Klusty, H. Wohltjen, Smart sensor system for trace organophosphorus and organosulfur vapor detection employing a temperature-controlled array of surface-acoustic-wave sensors, automated sample preconcentration, and pattern-recognition, Anal. Chem. 65 (1993) 1868–1881.
[6] G.A. Eiceman, J. Gardea-Torresday, E. Overton, A. Bhushan, H.P. Dharmasena, Gas chromatography, Anal. Chem. 78 (2006) 3985–3996.
[7] W.A. Bryden, R.C. Benson, H.W. Ko, M. Donlon, Universal agent sensor for counterproliferation applications, Johns Hopkins Apl Techn. Dig. 18 (1997) 302–308.
[8] G.L. Gresham, G.S. Groenewold, A.D. Appelhans, J.E. Olson, M.T. Benson, M.T. Jeffery, B. Rowland, M.A. Weibel, Static secondary ionization mass spectrometry and mass spectrometry/mass spectrometry (MS^2) characterization of the chemical warfare agent HD on soil particle surfaces, Int. J. Mass Spectrom. 208 (2001) 135–145.
[9] C.E. Kientz, Chromatography and mass spectrometry of chemical warfare agents, toxins and related compounds: state of the art and future prospects, J. Chromatogr. A 814 (1998) 1–23.
[10] E.J. Staples, S. Viswanathan, Ultra-high speed chromatography and virtual chemical sensors for detecting explosives and chemical warfare agents, IEEE Sensors J. 5 (2005) 622–631.
[11] W.E. Steiner, S.J. Klopsch, W.A. English, B.H. Clowers, H.H. Hill, Detection of a chemical warfare agent simulant in various aerosol matrixes

by ion mobility time-of-flight mass spectrometry, Anal. Chem. 77 (2005) 4792–4799.
[12] D.C. Collins, M.L. Lee, Developments in ion mobility spectrometry-mass spectrometry, Anal. Bioanal. Chem. 372 (2002) 66–73.
[13] G. Liu, Y. Lin, Electrochemical sensor for organophosphate pesticides and nerve agents using zirconia nanoparticles as selective sorbents, Anal. Chem. 77 (2005) 5894–5901.
[14] M.H. Hammond, K.J. Johnson, S.L. Rose-Pehrsson, J. Ziegler, H. Walker, K. Caudy, D. Gary, D. Tillett, A novel chemical detector using cermet sensors and pattern recognition methods for toxic industrial chemicals, Sensors Actuator B: Chem. 116 (2006) 135–144.
[15] A.A. Tomchenko, G.P. Harmer, B.T. Marquis, Detection of chemical warfare agents using nanostructured metal oxide sensors, Sensors Actuator B-Chem. 108 (2005) 41–55.
[16] D.S. Lee, H.Y. Jung, J.W. Lim, M. Lee, S.W. Ban, J.S. Huh, D.D. Lee, Explosive gas recognition system using thick film sensor array and neural network, Sensors Actuator B-Chem. 71 (2000) 90–98.
[17] S.W. Zhang, T.M. Swager, Fluorescent detection of chemical warfare agents: Functional group specific ratiometric chemosensors, J. Am. Chem. Soc. 125 (2003) 3420–3421.
[18] T.M. Swager, J.H. Wosnick, Self-amplifying semiconducting polymers for chemical sensors, MRS Bullet. 27 (2002) 446–450.
[19] S. Bencic-Nagale, T. Sternfeld, D.R. Walt, Microbead chemical switches: an approach to detection of reactive organophosphate chemical warfare agent vapors, J. Am. Chem. Soc. 128 (2006) 5041–5048.
[20] T.E. Mlsna, S. Cemalovic, M. Warburton, S.T. Hobson, D.A. Mlsna, S.V. Patel, Chemicapacitive microsensors for chemical warfare agent detection and toxic industrial chemical detection, Sensors Actuators B-Chem. 116 (2006) 192–201.
[21] S. Semancik, R.E. Cavicchi, M.C. Wheeler, J.E. Tiffany, G.E. Poirier, R.M. Walton, J.S. Suehle, B. Panchapakesan, D.L. DeVoe, Microhotplate platforms for chemical sensor research, Sensors Actuators B-Chem. 77 (2001) 579–591.
[22] D.C. Meier, C.J. Taylor, R.E. Cavicchi, E. White V, S. Semancik, M.W. Ellzy, K.B. Sumpter, Chemical warfare agent detection using MEMS-compatible microsensor arrays, IEEE Sensors J. 5 (2005) 712–725.
[23] T.A. Kunt, T.J. Mcavoy, R.E. Cavicchi, S. Semancik, Optimization of temperature programmed sensing for gas identification using micro-hotplate sensors, Sensors Actuator B-Chem. 53 (1998) 24–43.
[24] G.F. Li, M. Josowicz, J. Janata, Electrochemical assembly of conducting polymer films on an insulating surface, Electrochem. Solid State Lett. 5 (2002) D5–D8.
[25] K.D. Benkstein, S. Semancik, Mesoporous nanoparticle TiO_2 thin films for conductometric gas sensing on microhotplate platforms, Sensors Actuator B-Chem. 113 (2006) 445–453.
[26] K.D. Benkstein, C.J. Martinez, G. Li, D.C. Meier, C.B. Montgomery, S. Semancik, Integration of nanostructured materials with MEMS microhotplate platforms to enhance chemical sensor performance, J. Nanoparticle Res., in press, available online at http://www.springerlink.com/content/w82780400g288652/?p=c471f8b9f2734c6088ab3de42a33b291&pi=0.
[27] C.J. Taylor, S. Semancik, Use of microhotplate arrays as microdeposition substrates for materials exploration, Chem. Mater. 14 (2002) 1671–1677.
[28] Operating principle of semiconductor-type gas sensors, http://www.figaro.co.jp/en/item2.html.
[29] Z. Boger, D.C. Meier, R.E. Cavicchi, S. Semancik, Rapid identification of chemical warfare agents by artificial neural network pruning of temperature-programmed microsensor databases, Sensor Lett. 1 (2003) 86–92.
[30] Z. Boger, Artificial neural networks – unlikely but effective tools in analytical chemistry, in: Z.A. Alfassi, Z. Boger, Y. Ronen (Eds.), Statistical Treatment of Analytical Data, Blackwell Publishing, Oxford, UK, 2005, pp. 172–262.
[31] Z. Boger, Z. Karpas, Use of neural networks for quantitative ion mobility spectrometric measurements, J. Chem. Inform. Comp. Sci. 34 (1994) 576–580.
[32] Z. Boger, R.E. Cavicchi, S. Semancik, Analysis of conductometric microsensor responses in a 36-sensor array by artificial neural networks modeling, in: D'Amico, Di Natale (Eds.), Proceedings of the 9th International Symposium on Olfaction and Electronic Nose, Aracne Editrice S.r.l., Rome 2003, pp. 135–140.
[33] This experiment used devices possessing a different geometry, smaller contact area and thinner films than the example shown in Fig. 6a, resulting in lower overall conductance measurements. Note that the target signal is expressed as a decrease in conductance, contrasting with the conductance increases measured upon exposure to higher CMMP concentrations. This outcome is likely a convolution of differences in device geometry and analyte flow rates between the two examples.
[34] Mention of these and any other commercial products is strictly for provision of proper experimental definition, and does not constitute an endorsement by NIST.
[35] R.O. Duda, P.E. Hart, D.G. Stork, Maximum-likelyhood and Bayesian parameter estimation, in: Pattern Classification, 2nd, John Wiley & Sons, Inc., New York, 2001, Ch. 3.8.2, pp. 117–121.
[36] C.J. Martinez, B. Hockey, C.B. Montgomery, S. Semancik, Porous tin oxide nanostructured microspheres for sensor applications, Langmuir 21 (2005) 7937–7944.

Biographies

Douglas C. Meier holds a BA in Chemistry from Northwestern University and a PhD in Chemistry from Texas A&M University, where he studied the chemical physics of model catalyst systems under the guidance of Professor D. Wayne Goodman. Dr. Meier was subsequently awarded a National Research Council Postdoctoral Research Associateship in the Process Sensing Group at the National Institute of Standards and Technology (NIST). Now a NIST Research Chemist, he applies surface chemistry and thin film science in the development of advanced chemical microsensor arrays.

Jon K. Evju was born in Oslo, Norway in 1967 and is a Research Chemist working in the Solid State Chemical Microsensor Program at the National Institute of Standards and Technology (NIST). After completing high school at Hartvig Nissen VGS in Oslo, he attended University of Wisconsin at River Falls and received his BS in Chemistry in 1992. He was awarded a PhD in Chemistry from University of Minnesota, Minneapolis in 2000, for his graduate work on organometallic compounds, performed under direction of Professor Kent R. Mann. Upon completion of his thesis research, he joined Professor W.H. (Bill) Smyrl's research group at University of Minnesota, Department of CEMS as a Postdoctoral Research Associate and led the *f*-NSOM project to improve the technique and achieve <50 nm lateral resolution in scanning electrochemical microscopy. He joined NIST as a Guest Researcher in 2001 and worked to develop surface modification techniques for microfluidic polymer devices. In 2003, he was hired by NIST and has since earned recognition and awards within NIST and the Department of Commerce for performing realistic gas sensing experiments and for scientific merits associated with lowering limits of detection for the microhotplate gas sensors.

Zvi Boger received his BSc and MSc degrees in Chemical Engineering from the Technion – Israel Institute of Technology. Since then, until his recent retirement, he was employed at the Nuclear Research Center – Negev in senior engineering, research and management positions. As a private consultant on computer control of processes he worked in major projects of world-class companies in the US, Australia and Israel, as well as a consultant to several Israeli start-up companies. He had sabbatical leaves at MIT, Sydney University, University of Maryland, US National Institute of Standards and Technology (NIST), and published more than 120 journal and conference papers. Zvi Boger is the president of the consulting companies OPTIMAL – Industrial Neural Systems Ltd., Israel, and Optimal Neural Informatics LLC, USA, providing artificial neural networks (ANN) modeling, consulting and implementation services for industrial, biomedical and commercial applications. He served on the board of directors of the Israel Institute of Chemical Engineering, an Israeli Government supported "incubator" of hightech start-up companies, and on the board of directors of several Israeli start-up companies. He is active in the development and the application of ANN modeling techniques in various fields of science and engineering. As a Guest Researcher at NIST, he was involved for several years in analyzing data generated by a sensitive "electronic nose" sensor array. His recent research in the Department of Information System Engineering, Ben-Gurion University, Be'er

Sheva, Israel, is directed to Computer Malware Detection, Bio-Medical Modeling and Bioinformatics Pattern Recognition.

Baranidharan Raman received his Bachelor of Engineering in Computer Science with distinction from the University of Madras in 2000, and the MS and PhD degrees in Computer Science from Texas A&M University in 2003 and 2005, respectively. He is currently a NIH/NIST joint post-doctoral fellow in the Laboratory of Cellular and Synaptic Neurophysiology (NICHD), and the Process Sensing Group (NIST). His research interests include combining computational and electrophysiological approaches to study neural computations especially olfactory signal processing, sensor-based machine olfaction, machine learning, intelligent systems and robotics, and dynamical systems.

Kurt D. Benkstein is a Research Chemist with the Chemical Science and Technology Laboratory at the National Institute of Science and Technology. He received his BS degree in Chemistry in 1995 from Iowa State University, and his MS and PhD degrees in Chemistry from Northwestern University in 1996 and 2000, respectively. He went to the National Renewable Energy Laboratory in 2000 as a postdoctoral researcher to study the relation between nanoparticle film morphology and electron transport in dyesensitized solar cells. In 2003, Dr. Benkstein joined the National Institute of Standards and Technology as a Research Chemist, to examine porous nanostructured materials as conductometric gas sensors on advanced microdevices.

Carlos J. Martinez was born in Rio Piedras, Puerto Rico in 1972. He graduated with a Bachelor Degree in Physics and Electronics from the University of Puerto Rico at Humacao. He spent a year in Los Alamos National Laboratory before starting his graduate studies. He graduated in 2001 with a PhD in Materials Science and Engineering from the University of Illinois at Urbana-Champaign, where he worked with Prof. Jennifer Lewis in the area of ceramic film formation. During the year following graduation, he worked on a project to study the phase behavior of binary colloidal systems with a large-size asymmetry. In 2003, he received a National Research Council Postdoctoral fellowship to work with Steve Semancik in the Process Measurements Division at the National Institute of Standards and Technology developing porous nanostructures for chemical sensing. Currently, he is a visiting scientist in Prof. David Weitz's group at Harvard University, where he is using microfluidics to develop sensor architecture to perform single cell extra-cellular measurements in drops and hydrogels. He will join the Materials Engineering Department faculty at Purdue University in August, 2007.

Christopher B. Montgomery began his career in 1983 with Petrarch Systems, Inc. as an Organosynthetic Chemist. He performed custom syntheses, provided technical service and analytical evaluations of novel silicones and silanes developed for the electronics, biomedical and aerospace industries. In 1994, he joined SAIC developing protocols for self-assembled silane monomolecular layer formation (SAMMS), enabling hippocampal neuronal networks on patterned organosiloxy-modified surfaces. In 1997, he accepted a position with Commonwealth Scientific Corp. as a process engineer. Using ion beam technology, he developed and evaluated dielectric, diamond, optical and magnetic vacuum thin films serving the data storage, telecommunications and biomedical communities. In 2000, he joined the National Institute of Standards and Technology (NIST) preparing conductometric gas microsensor platforms. This includes micro-machining of the microhotplate structure, as well as tailoring surface properties for adhesion, electrical conductivity and catalysis via magnetron and ion beam sputtering. In addition, he performs vacuum thin-films research for fabricating or modifying a variety of micro-electromechanical devices.

Steve Semancik is the Project Leader of the Chemical Microsensor Program at the National Institute of Standards and Technology (NIST) in Gaithersburg, MD. He received his BS degree in physics from Rensselaer Polytechnic Institute and his MSc and PhD degrees, also in physics, from Brown University. Dr. Semancik's professional research career began as a National Research Council Postdoctoral Fellow, and has been centered in the fields of surface science and sensor science. His recent work has focused on developing improved nanomaterials for chemical sensing and combining such high performance materials with micromachined platforms to realize advanced microsensor devices and operating modes. Dr. Semancik has been elected as a Fellow of both the American Physical Society and AVS (formerly the American Vacuum Society) and is a Member of the Editorial Board of two sensor journals. He has authored or coauthored 125 papers (including four reviews), one book chapter, and five patents. Dr. Semancik has been the recipient of a number of awards, including the Chemical Science and Technology Laboratory Technical Achievement Award at NIST, and the US Department of Commerce Bronze and Silver Medals.